Magneto-conductance in open billiards: comparison between circle and stadium

1994 J. Phys. A: Math. Gen. 27 5889

(http://iopscience.iop.org/0305-4470/27/17/021)

J. Phys. A: Math. Gen. 27 (1994) 5889–5896. Printed in the UK

Magneto-conductance in open billiards: comparison between circle and stadium

K Nakamura, K Ito and Y Takane
Department of Applied Physics, Osaka City University, Osaka 558, Japan

Received 12 April 1994

Abstract. A comparative study is presented on quantum transports in weakly opened circle and stadium billiards in the perpendicular magnetic field B. While in the circle the magneto-conductance $g(B)$ shows grossly regular oscillations, in the stadium it exhibits a transition from mild to violent undulations with increase of B. The rich fluctuation features of $g(B)$, characterized by gradients of the cusp-like central peaks in autocorrelation functions, are attributed to the stability and instability of phase space in the underlying classical dynamics.

1. Introduction

Recent progress in fabrication of nanoscale or mesoscopic structures has formed a bridge between high technology and fundamental researches of nonlinear dynamics [1]. Both concave and convex billiards, around which studies of chaos are being accumulated, can be fabricated at the interface layer of semiconductor heterojunctions, e.g. GaAs/AlGaAs. Striking experiments by Marcus *et al* [2] indicated a crossover from aperiodic to periodic fluctuations of conductances in an open stadium billiard in a magnetic field.

Among concave billiards, the Bunimovich's stadium billiard has received a wide attention as a paradigm of nonlinear dynamics [3]. It belongs to the fully chaotic K system and, together with the kicked rotator, constitutes a prototype of conservative chaotic systems. Its quantum-mechanical study showed GOE level statistics [4] and periodic-orbit scars in wavefunctions [5], thereby heralding a new era of quantum chaos [6]. In the presence of a perpendicular magnetic field, the stadium billard becomes a generic system. Meplan *et al* 's treatment [7] elucidated its characteristic classical features: the erratic and ergodic phase space in a low field region is replaced by KAM tori via transitional unstable regions with increase of the field strength, in contrast to the circle billiard where the phase space is always occupied by periodic and non-ergodic orbits.

All these theoretical treatments, however, have been limited to a closed system without any leaky region and, with a few exceptions, little attention has been given to corresponding studies on its open-system version. Some prior works deserve mention: Jalabert *et al*'s works [8] include a study on open stadium billiards. Their openings are, however, made by suppressing the complete line segments of closed stadium and thus there is no way to bridge integrable circle and fully chaotic stadium by tuning the aspect ratio. Further, although both the semiclassical theory and the tight-binding calculations with Peierls' substitution are presented by this group, the former cannot incorporate the effect of diffraction at holes of billiards, and the latter spoils the salient aspect of the non-separability in non-integrable and chaotic systems. A recent paper by Wang *et al* [9] treated the open stadium with the same wire geometry as in [2]. They scrutinized, however, nothing about the quantum analogue of

0305-4470/94/175889+08$19.50

the transition from chaos to tori. Since they concentrated on a strongly opened case where the incident electron escapes to wires without significant collisions with the wall, it is not feasible to address the transition to be uncovered below by us. To our knowledge, therefore, the difference between magneto-conductances in weakly opened circle and stadium billiards is far from obvious.

In this paper, we present quantum and classical theories on the transports in open concave billiards in a perpendicular magnetic field. A pair of semi-infinite lead wires $j = 1$ and 2 are joined to the leaky holes of the billiard on its right and left sides, respectively (see figure 1(*b*)). (Although this wire geometry is different from that in [2], qualitative features of the magneto-conductance do not depend on it. The wire geometry in this paper was also used in [10].) This open system is characterized by a, b and d for semicircle radius, line segment length and width of holes at $x = a'_j = (-1)^j a'$, respectively, taking the origin at the centre of the billiards. Note $a' = b/2 + (a^2 - d^2/4)^{1/2}$. We shall choose the stadium with $b = 2a$ when the maximum Lyapunov exponent is available [3] and the circle with $b = 0$, while keeping fixed the area of the billiard $\mathcal{A}(= \pi a^2 + 2ab)$ and the degree of opening $d/\mathcal{A}^{1/2} = 0.1497$ common to both types. (In this case, $d/(2a) = 0.2$ and 0.1327 for the stadium and circle, respectively.) This degree corresponds to a *weakly opened situation* suitable to uncover the ample fluctuation properties of quantum transport. We shall be concerned with tuning the strength of the magnetic field. For convenience, the circle and stadium will be abbreviated as Cl and Sd, respectively. The region inside the billiard wall and within $|x| < a'$ will be prescribed as the cavity region. Nonlinear dynamics of electrons in this region will have a very significant effect on the S-matrix and quantum transports, and our major interest lies in this effect.

2. Quantum-mechanical treatment

For brevity, suppose the field B applies only to the cavity region, with no field in the wire regions. The essential quantities are cyclotron frequency and magnetic length given by $\omega = eB/m$ and $l_c = (\hbar/(eB))^{1/2}$, respectively. We choose the gauge potential in the Landau gauge, $\boldsymbol{A} = (0, -Bx, 0)$, which continuously changes to the constant value $\boldsymbol{A} = (0, -Ba'_j, 0)$ at the wires.

For an electron with the Fermi energy $E = (\hbar k_F)^2/2m$, the wavefunction Ψ satisfies the Schrödinger equation

$$(2m)^{-1}[-i\hbar\nabla + eA(\boldsymbol{r})]^2\Psi(\boldsymbol{r}) = E\Psi(\boldsymbol{r}). \tag{1}$$

For the incident propagating mode n at the wire 1, $\Psi(\boldsymbol{r})$ at wires $j = 1$ and 2 is written in terms of the S-matrix $\{S^{(j)}_{mn}\}$ as

$$\Psi^{(j)}(x, y; n) = \delta_{j1}\exp[ik_n(x - a'_j)]\phi_n(y) + \sum_{m=1}^{M} S^{(j)}_{mn}\exp\{(ieBa'_j/\hbar)y\}\exp[(-1)^j ik_m(x - a'_j)]\phi_m(y) \tag{2}$$

with the transverse component

$$\phi_m(y) = (2/d)^{1/2}\sin\{(m\pi/d)(y + d/2)\}. \tag{3}$$

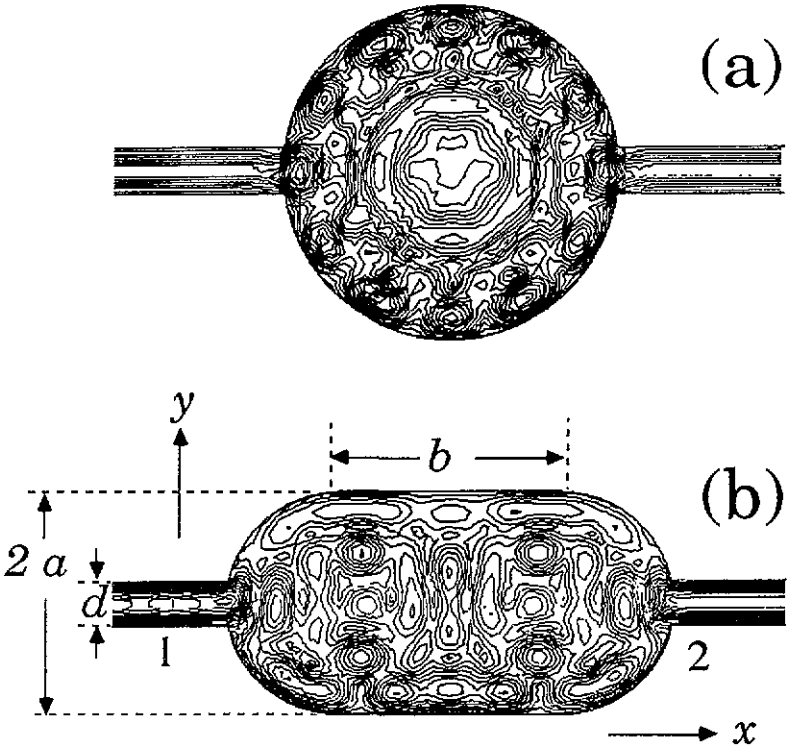

Figure 1. Contour map for wavefunctions $|\Psi|$ in the case of complete transmission: (*a*) circle with $B/B_0 = 12.2604$; (*b*) stadium with $B/B_0 = 12.6489$.

Here the wavevector is defined by $k = (k_m, m\pi/d)$ with $m\pi/d$ and $k_m = [k_F^2 - (m\pi/d)^2]^{1/2}$ for the transverse and longitudinal components, respectively. Modes m for $m \leqslant N$ and for $m > N$ with $N = [k_F d/\pi]$ correspond to propagating and evanescent waves, respectively.

In the cavity region, on the other hand, the Green function is given by [11, 12]

$$G(r, r'; \varepsilon) = (-m\pi/(2\pi\hbar^2))\{\exp[\mathrm{i}(x'y - xy' + xy - x'y')/2l_c^2]\} \times [(\cos\pi\varepsilon)\Gamma(\varepsilon + 1/2)]^{-1} W_{\varepsilon,0}(z)/z^{1/2} \tag{4}$$

where $\varepsilon = (E + \mathrm{i}\delta)/\hbar\omega$ is a scaled energy and $W_{\varepsilon,0}$ is the Whittaker function of $z(= |r - r'|^2/(2l_c^2))$.

To determine the values for S-matrix, we exploit Green's theorem which yields an equation including integrations along the closed boundary C of the cavity region:

$$\frac{\theta(r)}{2\pi}\psi(r) = -\frac{\hbar^2}{2m}\mathcal{P}\oint_C \left[G(r, r')\frac{\partial\psi(r')}{\partial n'} - \psi(r')\frac{\partial G(r, r')}{\partial n'}\right] \mathrm{d}S' - 2\frac{\mathrm{i}\hbar e}{2m}\mathcal{P}\oint_C G(r, r')A(r')\cdot n'\psi(r')\,\mathrm{d}S' \tag{5}$$

where r and r' lie on C and $\partial/\partial n'$ means outward-normal derivative. $\mathcal{P}$ and $\theta(r)$ denote Cauchy's principal value and the interior angle at r, respectively.

We shall here apply the boundary element method: the boundary of the cavity region is approximated by a sequence of small line segments. Then functions in the integrand along each integration segment in (5) are approximated by their linear interpolations: for a segment connecting r_i and r_{i+1}, for instance,

$$\begin{aligned} r(\xi) &= F_1(\xi)r_i + F_2(\xi)r_{i+1} \\ \Psi(r(\xi)) &= F_1(\xi)\Psi_i + F_2(\xi)\Psi_{i+1} \\ \partial\Psi(r(\xi))/\partial n' &= F_1(\xi)\partial\Psi_i/\partial n' + F_2(\xi)\partial\Psi_{i+1}/\partial n' \end{aligned} \tag{6a}$$

where

$$F_1(\xi) = (1-\xi)/2 \qquad F_2(\xi) = (1+\xi)/2 \tag{6b}$$

with $-1 < \xi < 1$. Substituting $G(r, r'; \varepsilon)$ in (4), its normal derivative and expressions in (6) into (5), we have

$$C_i\Psi_i = \sum_{l=1}^{N} P_{il}\Psi_l - \sum_{l=1}^{N} Q_{il}\partial\Psi_l/\partial n' \qquad (1 \leqslant i \leqslant N) \tag{7}$$

where C, P and Q are numerical coefficients and the boundary condition $r_{N+1} = r_1$ is imposed. Among unknown variables Ψ and $\partial\psi/\partial n'$, $\Psi = 0$ is satisfied at the wall, and Ψ and $\partial\psi/\partial n'$ at the holes $j = 1$ and 2 are rewritten in terms of S-matrix as

$$\Psi^{(j)}(a_j', y; n) = \delta_{j1}\phi_n(y) + \sum_{m=1}^{M} S_{mn}^{(j)} \exp\{(ieBa_j'/\hbar)y\}\phi_m(y) \tag{8a}$$

$$\partial\Psi^{(j)}(a_j', y; n)/\partial n' = -ik_1\delta_{j1}\phi_n(y) - \sum_{m=1}^{M} S_{mn}^{(j)}(-1)^j(ik_m)\exp\{(ieBa_j'/\hbar)y\}\phi_m(y). \tag{8b}$$

Using these notions in (7), we eventually obtain a set of linear equations for unknown variables $S^{(1)}$, $S^{(2)}$ and $\partial\psi/\partial n'|_{\text{wall}}$, whose solutions lead to the flux-normalized transmission coefficient $t_{mn} = (k_m/k_n)^{1/2}S_{mn}^{(2)}$ and the magneto-conductance

$$g(B) = (2e^2/h)\sum_{1\leqslant n,m\leqslant N} |t_{mn}|^2.$$

Similarly, wavefunctions are available by substituting the solution for $S^{(j)}$ and $\partial\psi/\partial n'|_{\text{wall}}$ into (5) with r taken inside the cavity region together with a new choice $\theta(r) = 2\pi$.

3. Numerical results

We concentrate on a single-mode ($N = 1$) injection by choosing $k_F d/\pi = 1.2$. Taking $B_0 = (h/e)/\mathcal{A}$ as a unit of the magnetic field, the scaled magnetic field B/B_0 will be varied between 1.72 and 27.62. (For a nanostructure with $a = 0.1$ μm, for instance, $\mathcal{A} = 7.14 \times 10^{-2}$ μm^2 and then $B_0 = 0.058$ T). In terms of Larmor radius $r_c(= \hbar k_F/(eB) =$

$(2\varepsilon)^{1/2}l_c$), this regime corresponds to $0.39 < r_c/a < 6.23$, which obviously covers both fully chaotic and transitional regions in the case of the Sd billiard [7].

Figure 1 shows the typical wavefunction features in the case of complete transmission. In the Cl billiard, $|\Psi|$ consists of structures with a partially broken circular symmetry (see figure 1(a)). The circularly-symmetric pattern changes regularly as B is varied. In the Sd billiard, in contrast, $|\Psi|$ shows no symmetric patterns (figure 1(b)), indicating the aperiodic variation of patterns with change of B. As seen below, this variation yields a rich structure of $g(B)$.

Figure 2 displays the conductance $g(B)$. Both billiard types commonly exhibit very noisy fluctuations, reminiscent of the universal conductance fluctuations in dirty metals. These anomalous fluctuations, regardless of integrability and non-integrability, are a typical feature of weakly opened systems where locations of highly concentrated S-matrix poles in the complex k plane are sensitive to the change of B field. Anomalous fluctuations of this kind were also reported on periodically-bended quantum wires [13].

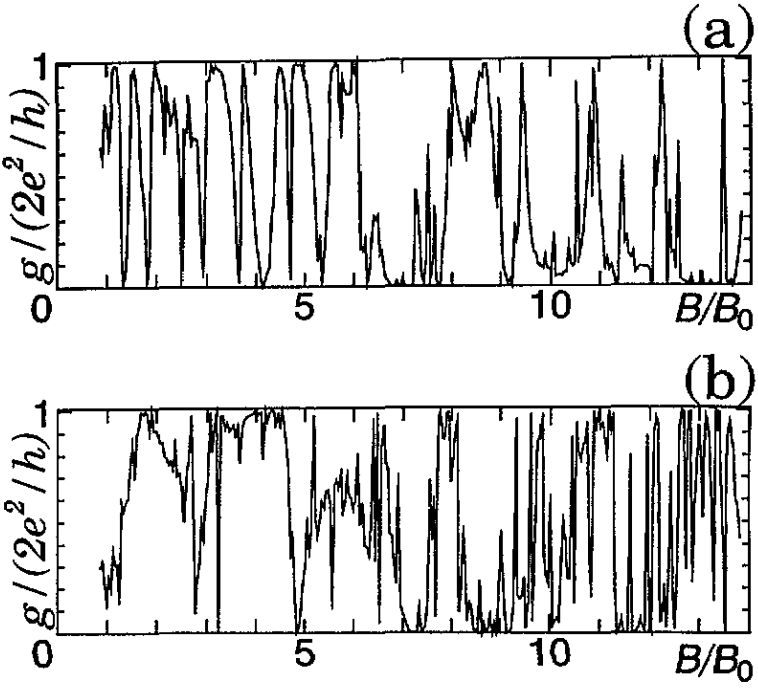

Figure 2. Quantum conductance $g(B)$: (a) circle; (b) stadium.

By a more careful insight, however, we find a clear difference between the two billiard types: in the Cl billiard, the frequency of fluctuations of $g(B)$ remains unchanged throughout the B-field range in figure 2(a). This result is consistent with the feature of the underlying classical dynamics where the phase space is occupied by tori whose structures are displaced regularly with the B field [7].

In the Sd billiard, in contrast, $g(B)$ exhibits slow and extremely rapid oscillations in the low and high field regions, respectively (figure 2(b)). The qualitative feature is in excellent agreement with the experiments by Marcus *et al* on a right-angled wire geometry [2]. The

threshold distinguishing the two distinct oscillations lies around $B/B_0 = 7.0$. This result can be understood by exploiting the structural stability of classical phase space. In fact, for $B < 7B_0$, $r_c > 1.53a$ and orbits are fully chaotic [7]. As a result the phase space is globally occupied by the ergodic sea whose feature is insensitive to the variation of B, consistent with the insensitivity of quantum transport. On the other hand, for $B > 7B_0$, the ergodic part begins, successively, to be replaced by KAM tori and thereby the phase space shows extreme sensitivity to the variation of B, which explains the rapid variation of $g(B)$.

To characterize the fluctuation of $g(B)$, the autocorrelation functions $\Gamma(\Delta B) = \langle \delta g(B)\delta g(B+\Delta B)\rangle_B / \langle (\delta g(B))^2 \rangle_B$ have been computed for both the low and high reference fields (figure 3). $\langle \bullet\bullet\bullet \rangle_B$ means the average over the referenced B fields. Both Cl and Sd billiards are commonly accompanied by cusp-like central peaks common to generic systems [14]. While for the Cl billiard (see figure 3(a)) the gradients of the cusps are the same in both of the low and high field regions, for the Sd billiard (see figure 3(b)) an obvious difference exists between the gradients in low and high reference fields: a long-range correlation and a rapid decrease of the correlation are obvious in the low field and high field regions, respectively.

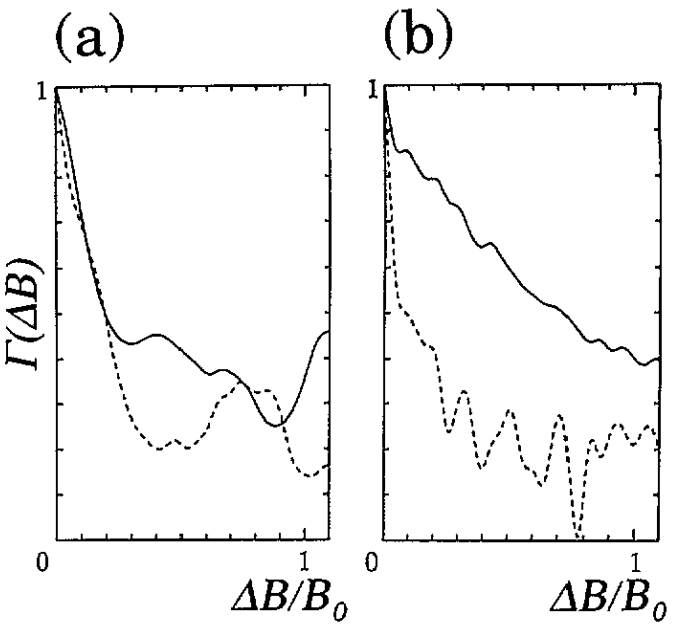

Figure 3. Autocorrelation functions $\Gamma(\Delta B)$. Reference ranges are $0 < B/B_0 < 7$ (solid line) and $7 < B/B_0$ (broken line): (a) circle; (b) stadium.

In order to see the quantum-classical correspondence, we shall calculate the classical conductance $g_{cl}(B)$: in accordance with the transverse component of the incident propagating mode in (2) and (3), an electron is supposed to lie initially at hole 1 with the occupation probability $|\phi_1(y)|^2$. We then compute its rate of escape to the wire 2 after significant classical bouncings with the wall and finally obtain $g_{cl}(B)$ in figure 4. For comparison, we also construct a smoothed version $g_{qt}(B)$ by coarse-graining of $g(B)$. (Smoothing is done here by averaging $g(B)$ over each interval of $\Delta B/B_0 = 0.1$ with successive intervals chosen by shifting the preceding one by $\Delta B/B_0 = 0.001$.) $g_{qt}(B)$

clearly shows the periodic (figure 4(*a*)) and aperiodic (figure 4(*b*)) alignment of peaks in the Cl and Sd billiards, respectively. $g_{cl}(B)$ reproduces the gross features of $g_{qt}(B)$. In particular the locations of peaks in g_{qt} are mostly identical to those of $g_{cl}(B)$ in both the Cl and Sd billiards except for the peaks around $B/B_0 = 5.5$ and 8.5 in figure 4(*a*). Thus the bouncing Larmor-orbit picture recovers the gross features of quantum conductance.

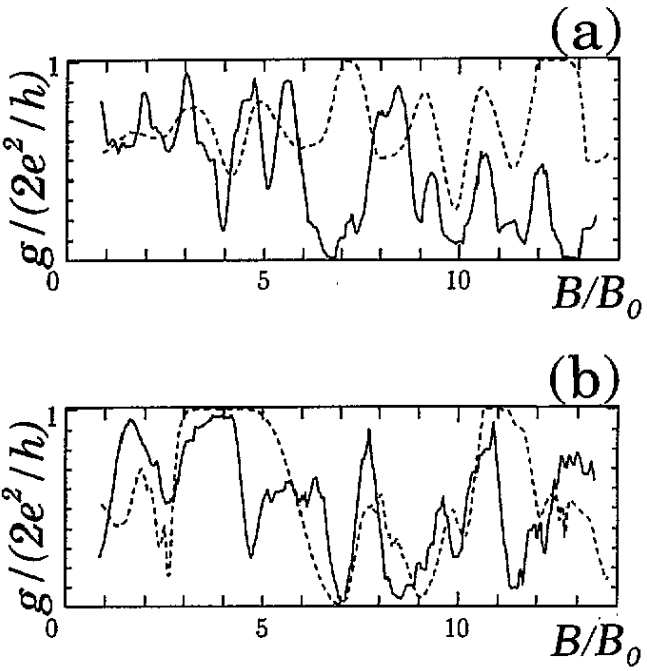

Figure 4. Coarse-grained quantum conductance g_{qt} (solid line) and classical conductance g_{cl} (broken line): (*a*) circle; (*b*) stadium.

4. Summary and conclusions

In conclusion, the magneto-conductance $g(B)$ in open Cl and Sd billiards is studied. It shows fluctuations dependent largely on the stability of phase space in the underlying classical dynamics of closed billiards. While in the Cl billiard the regular modulation of periodic orbits in the phase-space structure gives rise to regular oscillations of $g(B)$, in the Sd billiard the global chaos and genesis of successive tori are responsible for slow and rapid variations of the quantum conductance, respectively. The gradient of the cusp-like central peaks in the autocorrelation function characterizes the rich fluctuation properties of $g(B)$. The present results are consistent with Marcus *et al* 's experiment on a different wire geometry. Further, using the bouncing Larmor-orbit picture, we have derived the classical conductance, which turns out to reproduce most of the locations of peaks in the coarse-grained version of $g(B)$.

Acknowledgments

The authors are grateful to C M Marcus, T Ogawa and T Ueta for valuable discussions.

References

[1] Beenakker C W and van Houten H 1991 *Solid State Physics: Advances in Research and Applications* ed H Ehrenreich and D Turnbull (New York: Academic)

[2] Marcus C M, Rimberg A J, Westervelt R M, Hopkins P F and Gossard A C 1992 *Phys. Rev. Lett.* **69** 506
Marcus C M, Westervelt R M, Hopkins P F and Gossard A C 1993 *Phys. Rev.* B **48** 2460; 1993 *Chaos* **3** 643

[3] Bunimovich L A 1974 *Func. Anal. Appl.* **8** 254
Benettin G and Strelcyn J M 1978 *Phys. Rev.* A **17** 773

[4] McDonald S W and Kaufman A N 1979 *Phys. Rev. Lett.* **42** 1189

[5] Heller E J 1984 *Phys. Rev. Lett.* **53** 1515

[6] Gutzwiller M C 1990 *Chaos in Classical and Quantum Mechanics* (Berlin: Springer)
Nakamura K 1993 *Quantum Chaos: A New Paradigm of Nonlinear Dynamics* (Cambridge: Cambridge University Press)
Doron E, Smilansky U and Frenkel A 1991 *Physica* **50D** 367
See, also, Giannoni M J, Voros A and Zinn-Justin J (ed) 1991 *Chaos and Quantum Physics, Proceedings of the NATO ASI Les Houches Summer School* August 1989 (Amsterdam: North-Holland)

[7] Meplan O, Brut F and Gignoux C 1993 *J. Phys. A: Math. Gen.* **26** 237

[8] Jalabert R A, Baranger H U and Stone A D 1990 *Phys. Rev. Lett.* **65** 2442
Baranger H U, DiVincenzo D P, Jalabert R A and Stone A D 1991 *Phys. Rev.* B **44** 10 637
Balanger H U, Jalabert R A and Stone A D 1993 *Chaos* **3** 665

[9] Wang Y, Wang J and Guo H 1994 *Phys. Rev.* B **49** 1928

[10] Nakamura K and Ishio H 1992 *J. Phys. Soc. Japan* **61** 3939

[11] Feynman R P and Hibbs A R 1965 *Quantum Mechanics and Path Integrals* (New York: McGraw-Hill)

[12] Ueta T 1992 *J. Phys. Soc. Japan* **61** 4314

[13] Vacek K, Okiji A and Kasai H 1993 *Phys. Rev.* B **48** 11 412

[14] Lai Y C, Blumel R, Ott E and Grebogi C 1992 *Phys. Rev. Lett.* **68** 3491